*Article*

# Effect of Cu-Doped Carbon Quantum Dot Dispersion Liquid on the Lubrication Performance of Polyethylene Glycol

Shusheng Liu [1], Xiuqian Yu [1], Enzhu Hu [1,*], Enhao Su [1], Yanjie Chen [1], Jianping Wang [1], Kunhong Hu [1], Yong Xu [1], Xianguo Hu [2,*] and Hua Zhong [1]

[1] School of Energy Materials and Chemical Engineering, Hefei University, Hefei 230601, China
[2] Institute of Tribology, Hefei University of Technology, Hefei 230009, China
* Correspondence: huez@hfuu.edu.cn (E.H.); xghu@hfut.edu.cn (X.H.)

**Abstract:** Energy saving and reduced consumption of key materials such as bearings in high-end equipment can be realized by synthesizing a new lubricating functional additive, copper-doped carbon quantum dot dispersion liquid (Cu-CQDs) via hydrothermal reaction with glycerol, cupric chloride dihydrate, and choline chloride as raw materials. The influence of the dispersion liquid containing Cu-CQDs nanoparticles on the lubricating properties of polyethylene glycol (PEG200) was investigated on a four-ball friction tester. The wear scars of steel balls after friction were analyzed using a scanning electron microscope accompanied by energy dispersive spectroscopy (SEM/EDS), photoelectron microscopy, and Raman spectroscopy. The results revealed the friction and wear mechanism of Cu-CQDs. Cu-CQDs dispersion liquid can significantly enhance the lubrication performance of PEG. The average friction coefficient of PEG containing 2.0 wt% Cu-CQDs dispersion liquid was 40.99% lower than that of pure PEG. The friction and wear mechanism can be ascribed to friction, inducing Cu-CQDs to participate in the formation of boundary lubricating film, resulting in a low friction coefficient and wear scar diameter.

**Keywords:** copper doping; carbon quantum dots; boundary lubricating film; friction and wear mechanism

## 1. Introduction

Nanoparticles have broad application prospects because of their unique nano-size effect and superior chemical properties [1]. Many kinds of nano-materials exist, including copper, silver, nickel, molybdenum disulfide, tungsten disulfide, graphite nanosheets, nanospheres, graphene, carbon nanotubes, and carbon quantum dots (CQDs), which can be divided into organic, inorganic, and metal-based nanoparticles. Nanoparticles have been widely used in real life as lubricant additives. Its excellent antifriction and anti-wear properties and unique self-healing ability are potential substitutes for traditional additives that meet the developing requirements of high-performance lubricants [2,3]. It is well known that a large amount of energy loss in industrial production is caused by friction and wear. Improved lubrication can save 30% of energy. Therefore, how to save energy and reduce consumption is the focus of tribology scientists. The use of superior lubricants with the proper functional additives can prolong the life of mechanical components and realize energy savings and reduced consumption [4,5]. He et al. [6] used it as a functional additive of N32 lubricating oil. The nano copper bearing function improved the lubricating film's wear resistance and played a good role in reducing friction and anti-wear. Qin et al. [7] investigated halloysite nanotubes as an oil-based additive to improve the anti-wear properties. The outstanding wear resistance of the surface lubricated by the calcined product is attributed to the faster and easier formation of a multilayer nanocrystalline tribo-film. Jiang et al. [8] investigated and compared the tribological behaviour of steel/steel surface lubricated by poly alpha olefin (PAO 6) oil containing $MoS_2$/h-BN hybrid nanoparticles. The formation of the tribo-film on the surface of the

tribo-pair resulted in a lower friction coefficient and wear rate. Lahouij et al. [9] have studied the influence of the crystal structure of IF-MoS$_2$ nanoparticles on the lubricating properties of the fullerenes added to a synthetic base oil. The good lubricating properties of poorly crystallized particles by their higher ability to exfoliate and to form rapidly a tribo-film made of h-MoS$_2$ sheets on the surfaces compared to the perfectly crystallized particles. Li et al. [10] reported that nano-Cu powder can significantly improve the lubrication performance of PEG. The tribological mechanism can be attributed to the formation of copper deposition film by nano-Cu, thereby reducing the friction coefficient and the wear of friction pairs.

As a new material in the carbon family, CQDs are usually mono-disperse spherical carbon nanomaterials with a size of less than 10 nm, which are new nanomaterials with various industrial application prospects [11,12]. The research on the tribology of CQDs is still in its infancy. CQDs have remarkable tribological properties and great potential to become green and efficient lubricating materials. Kumar et al. [13] studied and introduced several applications, development progress, antifriction performance, anti-wear performance, and lubrication mechanism of lubricant additives based on carbon quantum dots (CQDs), and provided some suggestions on complete functionalized or mixed doped CQDs materials. Tang et al. [14] made a comprehensive and systematic review of the research progress of carbon dots in the lubrication field. The research work of carbon dots in the field of lubricating functional additives and lubricating coatings has been described in detail. Three strategies for improving the lubricating effect (size and shape control, surface modification, and heteroatom doping) have been pointed out, and the lubricating mechanism of CQDs and the main challenges have been comprehensively analyzed. Ma et al. [15] studied that CQDs and ionic liquid (IL) nanoparticles prepared by simple modification showed excellent tribological properties as lubricating materials and obtained a super-low friction coefficient of about 0.006 and wear rate of about $0.7 \times 10^{-14}$ m$^3$/Nm with the CQDs content of 3.6 wt%. The results show that IL-modified CQDs can provide a new idea for studying various lubricating materials to achieve ultra-low friction and can further study other practical applications. Shang et al. [16] studied chemically grafted CQDs and IL hybrid nanomaterials (CQDs/IL), and the hybrid nanomaterials with spherical shell structure showed a synergistic effect in improving the friction reduction and anti-wear properties of boundary lubrication. Tang et al. [17] found that the introduction of 0.1 wt% CQDs in water reduced the friction coefficient and wear rate by 33% and 80%, respectively. This finding can be attributed to the excellent tribological energy of CQDs from minimizing CQD sediment particles and reducing friction and wear through nano-bearing and nano-filling mechanisms. Hu et al. [18] prepared water-soluble CQDs by adjusting the carbonation degree of ammonium citrate through a simple, low-cost bottom-up method. The lubricity and inhibition of CQDs as nano-additive of water-based lubricant were studied. CQDs as environment-friendly nano-additives have low friction coefficients, excellent wear resistance, and excellent inhibition effect.

Limited studies have focused on the tribological properties of element-doped or hybrid CQDs. He et al. [19] prepared a new type of nitrogen-doped CQD (N-CQD) nanoparticles by solvothermal method. The particle diameter is about 10 nm. Nanoparticles have a graphene oxide (GO) micro graphitization structure, and they were added to MoS$_2$ nanofluids. The tribological properties of the composite fluid were investigated, and the results show that the friction process of MoS$_2$ and N-CQDs nanofluids was in a mixed lubrication state. The particles do not interfere with each other and play a synergistic role in lubrication. Ye et al. [20] studied nitrogen-doped CQDs (N-CQDs) as functional additives and explored their influence on the lubricating properties of bio-based castor oil. The chemical grafting of CQDs in the olefins (PAO) with good dispersion. The friction mechanism can be attributed to the continuous deposition of the wear surface by nanoparticles at the interface of the friction pair, forming a thin protective film containing iron oxide, inorganic carbon, and nitrogen. Tu et al. [21] synthesized a new green lubricating oil additive CQDs particle-doped nickel (Ni-CQDs) with citric acid and nickel acetate as raw materials. The effects

of CQDs and Ni-CQDs nanoparticles on the friction behaviour of polyethylene glycol (PEG200) were investigated. Results show that both CQDs and Ni-CQDs particles can enhance the lubrication performance of PEG200. Moreover, Ni-CQDs nanoparticles can enhance the lubricating performance compared with ordinary CQD particles. This finding can be attributed to the fact that friction induces Ni-CQDs to participate in the formation of friction film, resulting in a low friction coefficient and wear rate. Huang et al. [22] found that when CQDs/CuSx nanocomposite particles are used as additives, they show excellent lubrication and superior repair ability of worn surfaces. The mechanism can be attributed to the combination of the multilayer graphite structure of CQDs and the high chemical activity of CuSx. Shang et al. [23] prepared a hybrid of CQDs and graphene oxide (GO) through a one-pot method. The tribological behaviour of PEG as a lubricating additive was studied. A significant antifriction effect was observed, and the mechanism can be attributed to the synergistic effect of adsorption of spherical CQDs and GOs on the sliding surface, which effectively protected the interface from bad friction and wear.

Limited research has focused on the preparation of metal-based biomass CQDs dispersion and its tribological properties. Therefore, the copper-doped CQDs dispersion was prepared using a traditional hydrothermal synthesis method, and the influence of different concentrations of the dispersion on the lubrication characteristics of PEG lubricant was investigated. The successful implementation of this work has laid a certain foundation for the development of high-performance lubricants and provided basic data for enriching the tribological research of metal-based CQDs.

## 2. Experimental

### 2.1. Preparation and Dispersion of Materials

2.1.1. Preparation of Copper-Doped CQDs Dispersion

Precursor solution (DES): Choline chloride (analytically pure, Shanghai Zhanyun Chemical Co., Ltd., Shanghai, China), cupric chloride dihydrate (analytically pure, Shanghai Zhanyun Chemical Co., Ltd.), and glycerol (analytically pure, Sinopharm Chemical Reagent Co., Ltd., Shanghai, China) were weighed at a proportion of 5:1:1, and the mixed solution was poured into a 50 mL three-necked flask and placed in an oil bath to prevent liquid splashing and water loss during heating. The bottle mouth was covered with a rubber stopper. At room temperature, the oil bath was stirred and heated to 110 °C, and the reaction lasted for 5 h until the precursor solution became stable. After the solution was cooled to room temperature, it was sealed for use.

Hydrothermal synthesis: Approximately 1.0 g of DES solution was obtained, mixed with 30 mL of pure water, placed in a beaker, and sealed. The mixture was stirred with small magnets for 2 h until the DES solution was uniformly dispersed in pure water. The sample was placed in mixed DES solution into a 50 mL reaction kettle lined with polytetrafluoroethylene, the shell was tightened, the oven temperature was set to 220 °C, and it was held for 24 h for the successful preparation of Cu-CQDs. After the reaction, 0.22 μ the supernatant was filtered out by PVDF membrane, and the macromolecular impurities were removed by dialysis with 3500D dialysis bag for 2 days. After rotary evaporation, the solution was freeze-dried to obtain copper-doped carbon dots dispersion.

2.1.2. The Mutual Solubility of Copper-Doped CQDs Dispersion with PEG200

The dispersion containing copper-doped carbon nanoparticles was added to the base oil PEG200 (99%, Shandong Yousuo Chemical Co., Ltd., Heze, China) as a lubricating additive. The dispersion characteristics of its nanoparticle dispersion with different mass fractions in PEG are shown in Figure 1. The figure that copper-doped carbon dots have good dispersion in PEG. The yield of copper-doped carbon nanoparticle dispersion is approximately 95.35%. The formation mechanism can be summarized as follows: during the formation of doped carbon dots, glycerol molecules, and cupric chloride molecules experienced a process of "Dispersion pyrolysis, Aggregation carbonization, Hydrothermal

recombination" three kinds of reaction processes [24]. The specific colour development mechanism can be expressed in publicity (1).

$$[Cu(H_2O)_4]^{2+} + 4Cl^- \leftrightharpoons (CuCl_4)^{2-} + 4H_2O, H > 0 \tag{1}$$
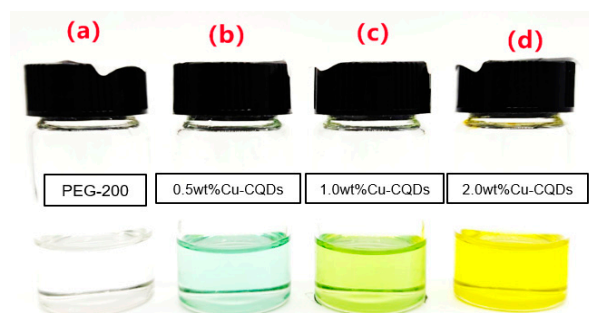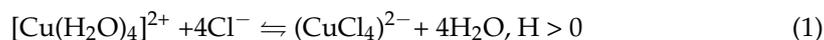


**Figure 1.** Mutual solubility of Cu-CQDs dispersions with different mass concentrations in PEG200.

Cu-CQD dispersions with different amounts of addition show different colours in PEG. The colour change mechanism can be explained as follows: After dissolution in PEG200, hydrated copper ions $[Cu(H_2O)_4]^{2+}$, and tetrachloride copper complex ions $[CuCl_4]^{2-}$ are formed by the combination of $Cl^-$ and copper ions. The colour of the ions is yellow, because the concentration of Cu-CQDs changes the equilibrium constant of copper tetrachloride ion, making it move forward. With the increase in concentration, the colour of the solution changed from blue to yellow-green and then yellow (Figure 1 shows the colour change of copper-based CQDs in PEG).

*2.2. Characterization of Physical and Chemical Properties of Cu-CQDs Particles in Dispersion Solution*

Transmission electron microscopy (TEM, FEI Tecnai 200 kV) was used to characterize the internal structure of the Cu-CQDs particles in the dispersion solution and the morphological characteristics of the primary particles. As shown in Figure 2a, the Cu-CQDs particles were uniformly dispersed, and the average particle size was approximately 8.33 nm. Then, a fluorescence spectrophotometer (Edinburgh FLS1000, EI) was used to obtain the fluorescence emission spectrum of copper-based carbon dots at the excitation wavelength of 360 nm and at room temperature. Figure S1 shows that the maximum emission wavelength of fluorescence is 525 nm, and the maximum emission wavelength does not change with time without a blue shift or red shift. The absorption spectrum of CQDs was measured using an ultraviolet–visible absorption spectrometer (UV-1800, Mapada). The dispersion of Cu-CQDs in water was conducted with Zeta spectroscopy (model Zs90). It indicated that Cu-CQDs particles could be dispersed uniformly as shown in Figure 2b,c shows that their absorption ranges are all in the ultraviolet light region, and relatively wide absorption peaks belonging to the near ultraviolet region were observed between 200–250 nm, which can be attributed to $\pi$-$\pi$ * transition of aromatic sp2 hybridization. The molecular structure of the material was characterized using a Fourier transform infrared spectrometer (NicoletiS50). The functional group absorption peak was inferred based on the vibration form of the molecular group corresponding to the absorption peak. As shown in Figure S2, the peak at 3357 cm$^{-1}$ of Cu-CQDs shown in Figure 2b is the absorption peak of -OH, the peak at 1636 cm$^{-1}$ is the absorption peak of C=O, and the peak at 1080 cm$^{-1}$ is the characteristic absorption peak of C-O stretching vibration in -C-OH [25,26]. PEG200 is a hydrophilic polymer with a large number of hydroxyl groups on its molecular surface, which makes it show polar properties and can be well compatible with Cu-CQDs, which is also the reason why PEG is selected as the base oil. Figure S2c shows the infrared spectrum of PEG200. The peak at 3405 cm$^{-1}$ is the absorption peak of -OH. In the figure, there is a strong absorption peak at 1062 cm$^{-1}$, which is the characteristic absorption peak of C-O-C stretching vibration in the PEG200 molecule. Figure 2a shows the infrared spectrum of the

added amount of 1.0 wt% Cu-CQDs in PEG200, the functional groups are almost the same as PEG due to the small proportion of the added amount.
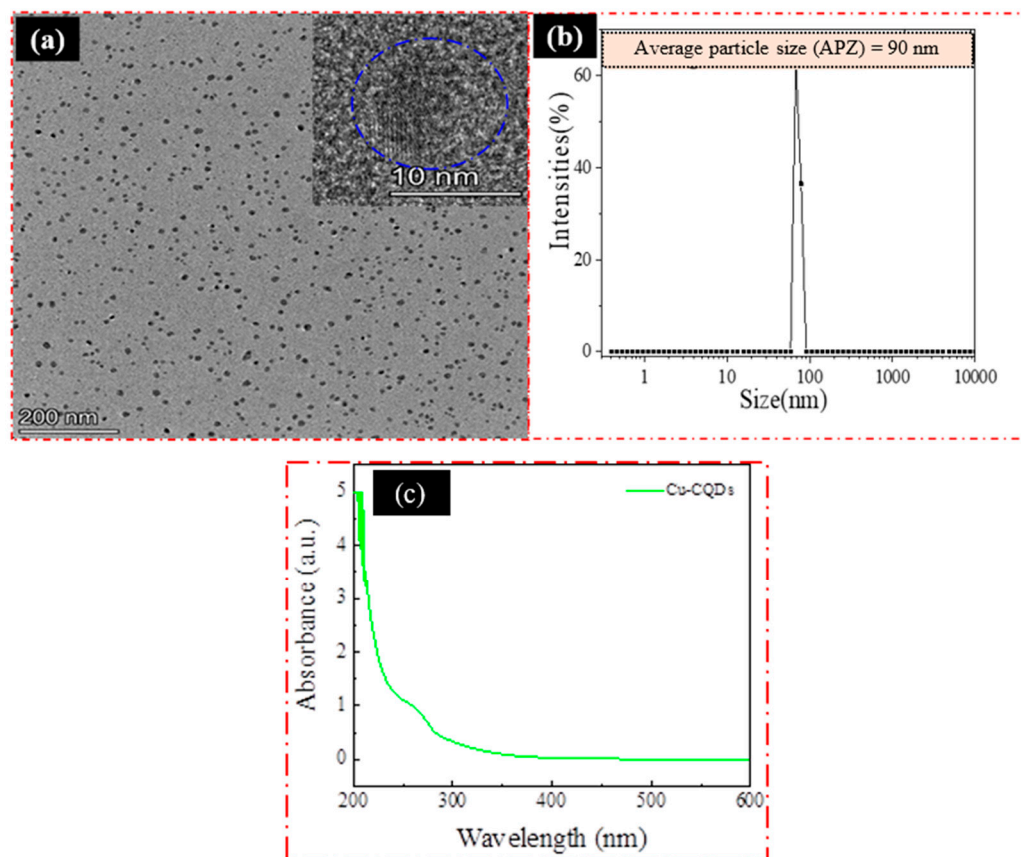


**Figure 2.** HRTEM, particle size distribution of Cu-CQDs in water and UV absorption spectrum of copper-doped carbon quantum dots. (**a**) TEM images of Cu-CQDs; (**b**) particle size distribution of Cu-CQDs in water; and (**c**) ultraviolet visible absorption spectrum.

### 2.3. Tribological Tests

The four-ball friction testing machine (MRS-10D type) is shown in Figure 3. Based on the petrochemical industry standard parameters of 392 N and 1200 rpm/min, the tribological test was carried out for 30 min at 25, 75, and 100 °C [27]. The GB/3142-2019 test standard was used to test the maximum seizure load ($P_B$ value, accuracy less than 10 N) of solution oils with different concentrations of Cu-CQDs. Table 1 provides the $P_B$ values of solution oils with different concentrations of Cu-CQDs. The four steel balls were arranged according to the regular tetrahedron, the upper ball rotated at 1450 ± 5 rpm/min, the lower three balls were fixed together with oil boxes, and the load was applied to the steel balls from bottom to top through the hydraulic system. During the test, the contact points of the four steel balls were immersed in the lubricant. Each test lasted for 10 s. After the test, the wear spot diameter of any steel ball in the oil tank was measured. The test was repeated according to the specified procedure until the evaluation index representing the bearing capacity of the lubricant was obtained [28].

The steel ball used in the test was ASTM E2100 bearing steel with a diameter of 12.7 mm, which was manufactured according to the Chinese national standard GB/T308-2002. The hardness of steel was set to HRC = 65, and the average surface roughness was Ra = 0.012 μm [29]. The lubrication state was reduced to the boundary lubrication condition by analysis of the friction coefficients of samples and surface contact stress of steel balls [30]. The antifriction and wear behaviours of Cu-CQDs as a lubricating additive under different working conditions were explored by subjecting all oil samples to ultrasonic dispersion treatment for

30 min. The test steel balls and oil box abrasives were cleaned with ethanol or petroleum ether. Each group of experiments was carried out thrice independently to reduce the experimental deviation [31,32]. SEM/EDS and a 3D laser scanning microscope (VK-X100k) were used to analyze the morphology of the wear scar area and the element composition on the surface. The valence states of chemical elements were studied by X-ray photoelectron spectroscopy (ESCALAB 250), and the mechanism of friction and wear was expounded.
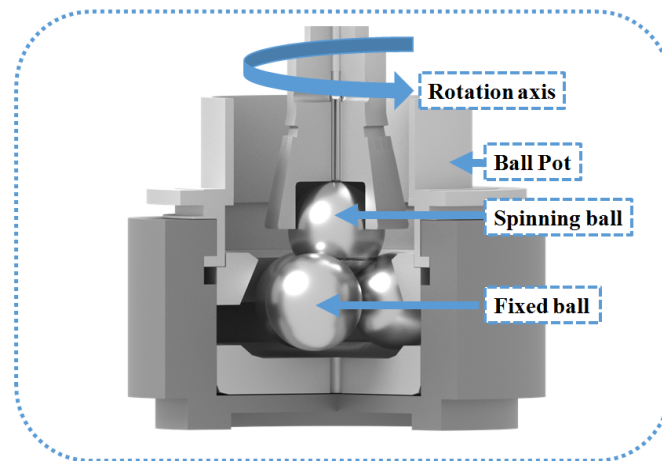


**Figure 3.** Schematic diagram of a four balls tribo-meter.

**Table 1.** $P_B$ value of solution oil with different concentrations of Cu-CQDs.

| Sample | Maximum Non-Seizure Load (N) | Rate of Change (%) |
|---|---|---|
| PEG200 | 530 | – |
| 0.5 wt% Cu-CQDs | 588 | 10.94% |
| 1.0 wt% Cu-CQDs | 588 | 10.94% |
| 2.0 wt% Cu-CQDs | 637 | 20.19% |

## 3. Results and Discussion

### 3.1. Antifriction Property

Figure 4 shows the influence of different amounts of dispersion on PEG lubrication characteristics at 25, 75, and 100 °C. As shown in Figure 4a, at 25 °C, with the increase in the content of Cu-CQD dispersion, the friction coefficient also decreased, with a maximum reduction of 19.83%, reflecting the Cu-CQDs can promote the antifriction property of PEG200. Figure 4b,c show the change in friction coefficient under the lubrication of different amounts of dispersion at 75 and 100 °C. With the increase in the content of Cu-CQD dispersion, the friction coefficient decreased. With the increase in temperature, the friction coefficient became considerably lower than that of pure PEG200. At 75 °C the highest reduction was 31.86%. At 100 °C, the maximum reduction was 40.99%. At high temperature, the lubricating performance of the oil sample was significantly enhanced, and the results are shown in Figure 4c,d. By using the formulas $\sigma = 1.5 \times W_1/(\pi \times a^2)$ [33], the contact surface stress between steel balls during lubrication ($W_1$ refers to the pressure between steel balls, and $a$ refers to the circular contact area between steel balls) can be calculated, and the results are shown in Table 2. Combined with the friction coefficients analysis of samples, which indicates that Cu-CQDs are in a boundary lubrication state when lubricated with PEG at different temperatures, friction can induce Cu-CQDs to participate in the formation of boundary lubrication film.
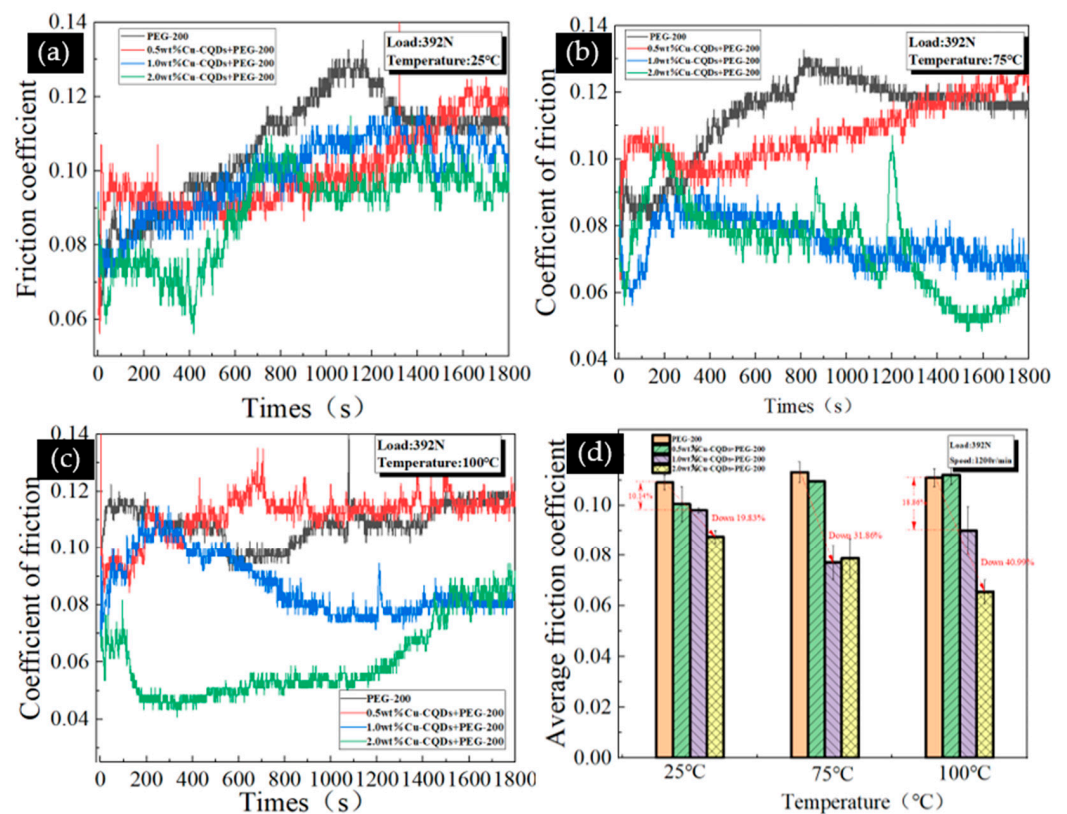
**Figure 4.** The changes of friction coefficients with different mass fractions of Cu-CQDs dispersion (1200 rpm/min, each group lasts for 30 min), (**a**) 25 °C; (**b**) 75 °C; (**c**) 100 °C; and (**d**) histogram of average friction coefficient under different working conditions.

**Table 2.** Contact surface stress of oil samples under different temperatures.

| Samples | 25 °C (Gpa) | 75 °C (Gpa) | 100 °C (Gpa) |
|---|---|---|---|
| PEG200 | 0.33 | 0.54 | 0.24 |
| 0.5 wt% Cu-CQDs | 0.51 | 0.47 | 0.37 |
| 1.0 wt% Cu-CQDs | 0.43 | 0.68 | 0.51 |
| 2.0 wt% Cu-CQDs | 0.41 | 0.36 | 0.29 |

*3.2. Abrasion Resistance Property*

Figure 5 shows the changes in average wear scar diameter (AWSD) under oil sample lubrication with different Cu-CQD dispersions at different temperatures. When the oil temperature was 25 °C the AWSD diameter of pure PEG200 was 0.71 mm. When Cu-CQD dispersions with different contents were added, AWSD decreased slightly. The oil film thickness of PEG possibly took an important role in reducing the AWSDs. However, when adding high contents of Cu-CQDs, the aggregation role resulted in the high AWSDs.

At 75 °C, the AWSD of pure PEG200 was 0.56 mm. When 1.0 wt% Cu-CQDs dispersion was added, the AWSD of the oil sample decreased significantly. Friction induced the formation of tribo-film including components of Cu-CQDs particles. Chemical reactions took place on the surfaces of steel balls during the friction process which is better than that of oil film thickness. The AWSD of pure PEG was 0.83 mm at 100 °C. When 0.1 wt% Cu-CQDs dispersion was added, the AWSD decreased to 0.57 mm, with a reduction rate of 31.2%. Cu-CQDs nanoparticles can significantly improve the anti-wear properties of base oil PEG200 at higher temperatures. However, with the increase in oil temperature from room temperature to 75 and 100 °C, when 2.0 wt% of Cu-CQDs was added, AWSD

is higher than that of other additions. After the tests, scratches of different degrees were found at the bottom of the steel balls. When a high concentration of Cu-CQDs was added to PEG200, a certain amount of Cu-CQDs nanoparticles or wear debris at the interface of the friction pair will agglomerate, and abrasive wear will occur at the interface of the friction pair, thus reducing the wear resistance property of PEG [34]. Friction film plays an important role in wear resistance. The optimal concentration of Cu-CQDs nanoparticles additive was 1.0 wt%. $P_B$ value in Table 1 also confirms the above experimental results, and Cu-CQDs nanoparticles had the most significant wear resistance at high temperatures.
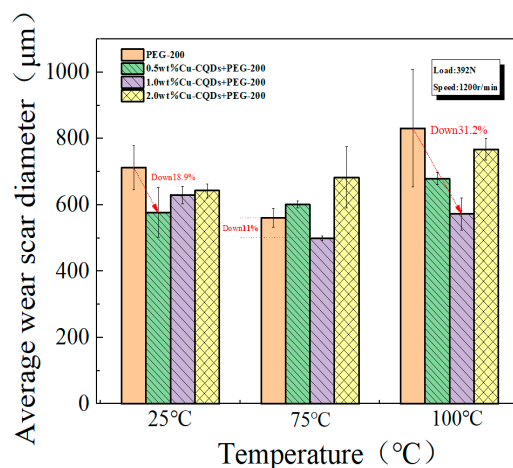


**Figure 5.** Change of average wear scar diameter under lubrication of Cu-CQDs dispersion with different mass fractions (1200 rpm/min, each group lasts for 30 min).

### 3.3. Surface Analysis

The micro-oil stain analysis system (YP-2 type) was used to analyze the oil stain after the experiment. Figure S3 shows the oil stain of 2.0 wt% Cu-CQDs at different temperatures. The oil stain was possibly composed of copper ion and chloride ion complexes, iron filings and iron oxides, and copper, and its derivatives. After friction, the wear debris and abrasive particles in the dispersion show agglomeration in Figure S3a, and the colour of the oil sample was significantly deepened in Figure S3c. Friction induced the oxidation of the oil.

Figures 6–8 show the cross-sectional area, three-dimensional morphology, average wear scar diameter, and its change rate of wear scar area lubricated by different oil samples at different temperatures. At 25 °C, many wide pits and deep grooves were observed on the surface of the steel ball, as indicated by the red arrow in Figure 6. This finding shows that the protection ability of pure PEG on the surface of steel balls is poor. When different amounts of Cu-CQDs were added, the width and depth of the furrow on the surface of the steel ball were significantly reduced, and the lubricating film formed. The average wear scar diameter on the steel ball surface decreased significantly. When 0.5 wt% Cu-CQDs was added, the AWSD decreased by 18.93% compared with pure PEG as shown in Figure 6. At 75 °C, under pure PEG lubrication, the surface furrow was very deep, but the average wear scar diameter slightly changed to approximately 560.72 μm. Different amounts of Cu-CQDs were added, and only 1 wt% Cu-CQDs reduced the average wear scar diameter by 11%, as shown in Figure 7. This conclusion can be attributed to the decomposition of PEG at 75 °C, resulting in the improvement of lubrication performance, and the lubrication efficiency is better than that of Cu-CQDs particles. At 100 °C, when 1.0 wt% Cu-CQDs was added to PEG, the wear spot diameter of the steel ball decreased by the largest proportion. In comparison with pure PEG lubrication (0.83 mm), the wear spot diameter decreased by 31.2%, as shown in Figure 8.

Figure 9 shows SEM/EDS analysis of the steel ball surface under different oil sample lubrication. Figure 9a shows a deep furrow on the surface of the steel ball lubricated by pure PEG, as indicated by the red arrow. This finding shows that PEG has a poor ability

to protect the surface of the steel ball. The energy spectrum analysis shows that the main elements on the surface are carbon, oxygen, and iron. When 0.5 wt% Cu-CQDs were added to PEG, the width of the furrow of the ink mark on the steel ball surface was significantly reduced, and the friction-induced boundary film on the surface was formed as shown by the red arrow (Figure 9b). The energy spectrum analysis of the wear mark area shows that, except for the steel ball component elements, the copper content was significantly increased, reaching 0.8 wt%. Therefore, the friction-induced copper-doped carbon dots participated in the composition of the boundary film. The furrow depth on the surface of the steel ball was significantly reduced, and the surface smoothness was significantly better than that of the sample without carbon dots when the steel ball was continuously added at contents of 1.0 and 2.0 wt%. The results also confirmed that the copper-doped carbon dots participated in the formation of boundary lubrication film and remarkably improved the lubrication characteristics of PEG200.
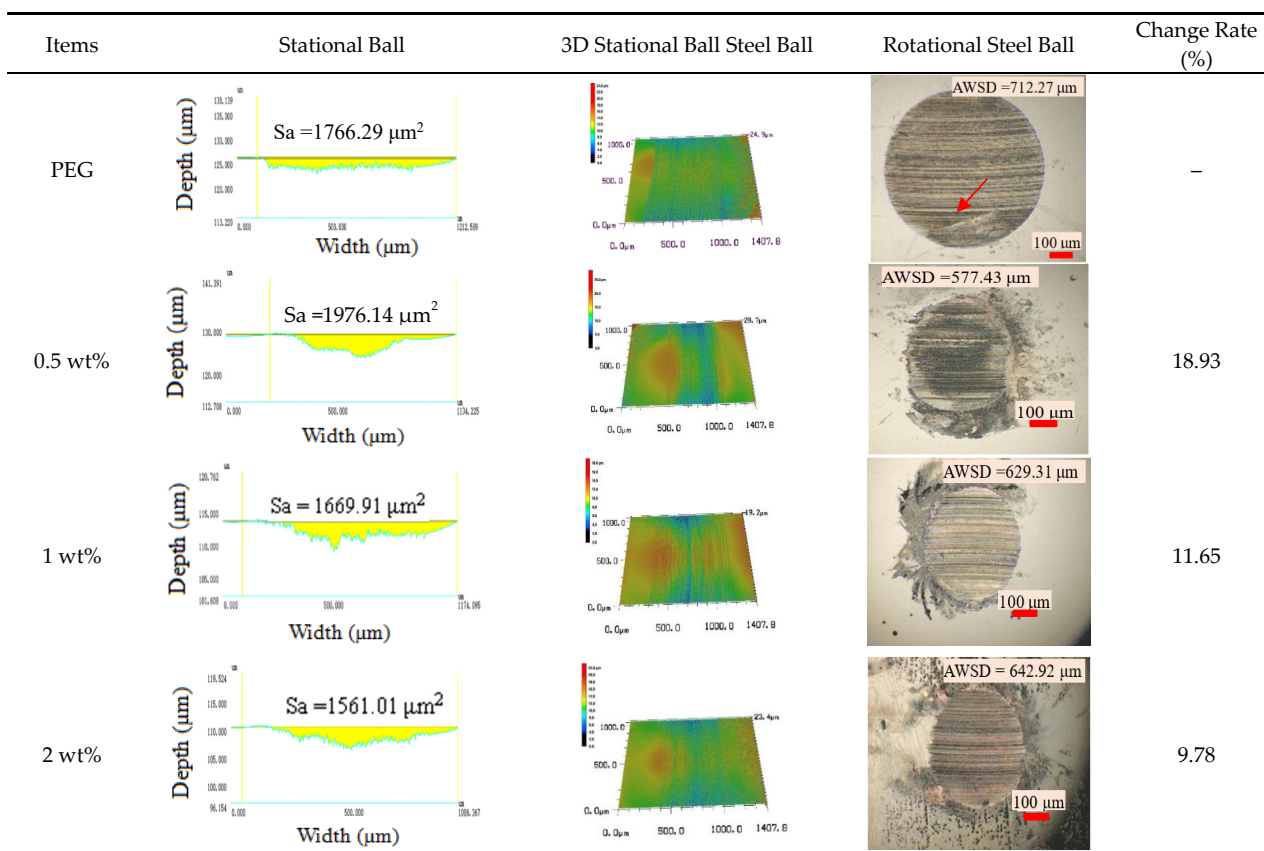
| Items | Stational Ball | 3D Stational Ball Steel Ball | Rotational Steel Ball | Change Rate (%) |
|---|---|---|---|---|
| PEG | $S_a$ =1766.29 $\mu m^2$ | | AWSD =712.27 $\mu m$ | – |
| 0.5 wt% | $S_a$ =1976.14 $\mu m^2$ | | AWSD =577.43 $\mu m$ | 18.93 |
| 1 wt% | $S_a$ = 1669.91 $\mu m^2$ | | AWSD =629.31 $\mu m$ | 11.65 |
| 2 wt% | $S_a$ =1561.01 $\mu m^2$ | | AWSD = 642.92 $\mu m$ | 9.78 |

**Figure 6.** Cross-sectional area, three-dimensional morphology, average wear scar diameter, and change rate of wear scar area lubricated by different oil samples at 25 °C.
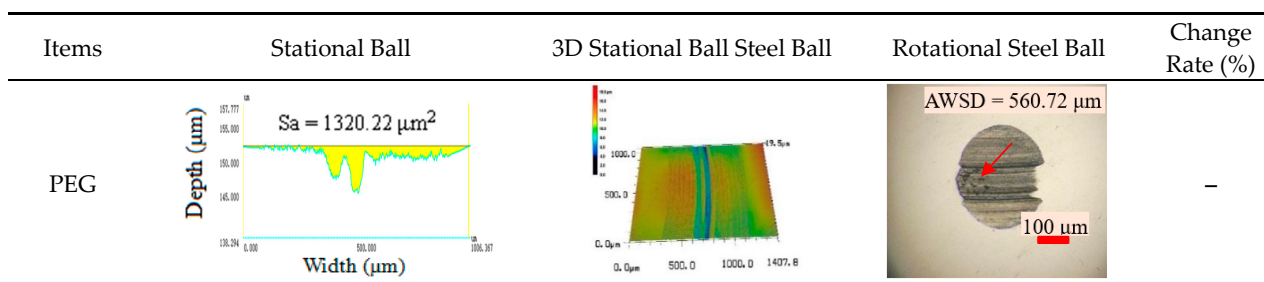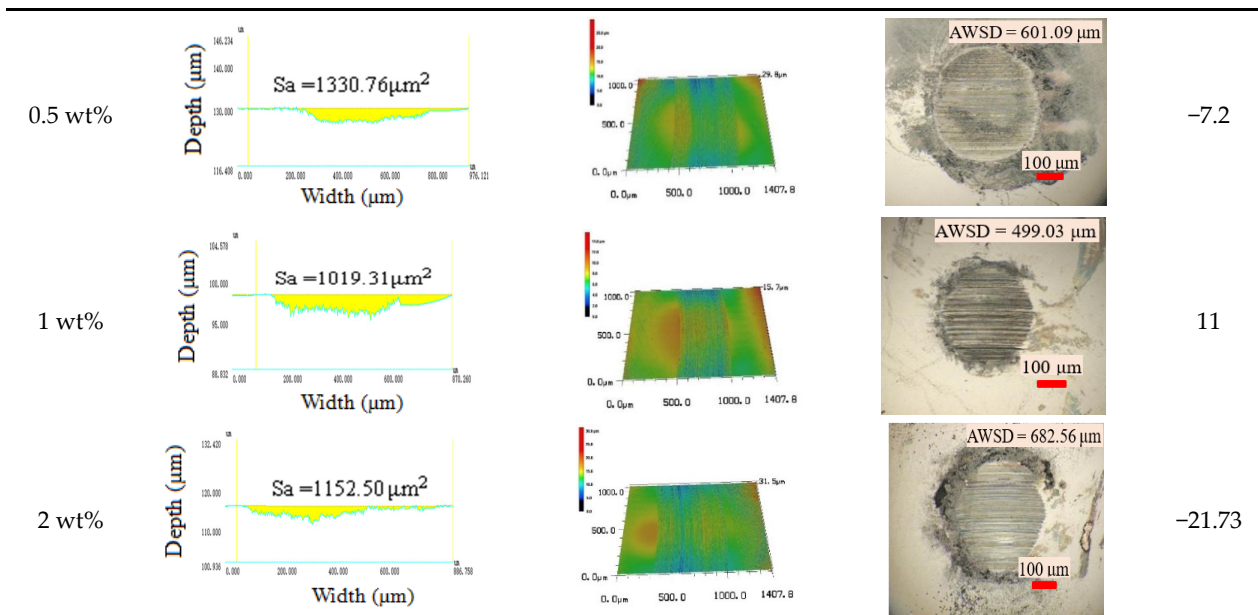
| Items | Stational Ball | 3D Stational Ball Steel Ball | Rotational Steel Ball | Change Rate (%) |
|---|---|---|---|---|
| PEG | $S_a$ = 1320.22 $\mu m^2$ | | AWSD = 560.72 $\mu m$ | – |

**Figure 7.** *Cont.*

| | | | | |
|---|---|---|---|---|
| 0.5 wt% | | | AWSD = 601.09 µm | −7.2 |
| 1 wt% | | | AWSD = 499.03 µm | 11 |
| 2 wt% | | | AWSD = 682.56 µm | −21.73 |

**Figure 7.** Cross-sectional area, three-dimensional morphology, average wear scar diameter, and change rate of wear scar area lubricated by different oil samples at 75 °C.
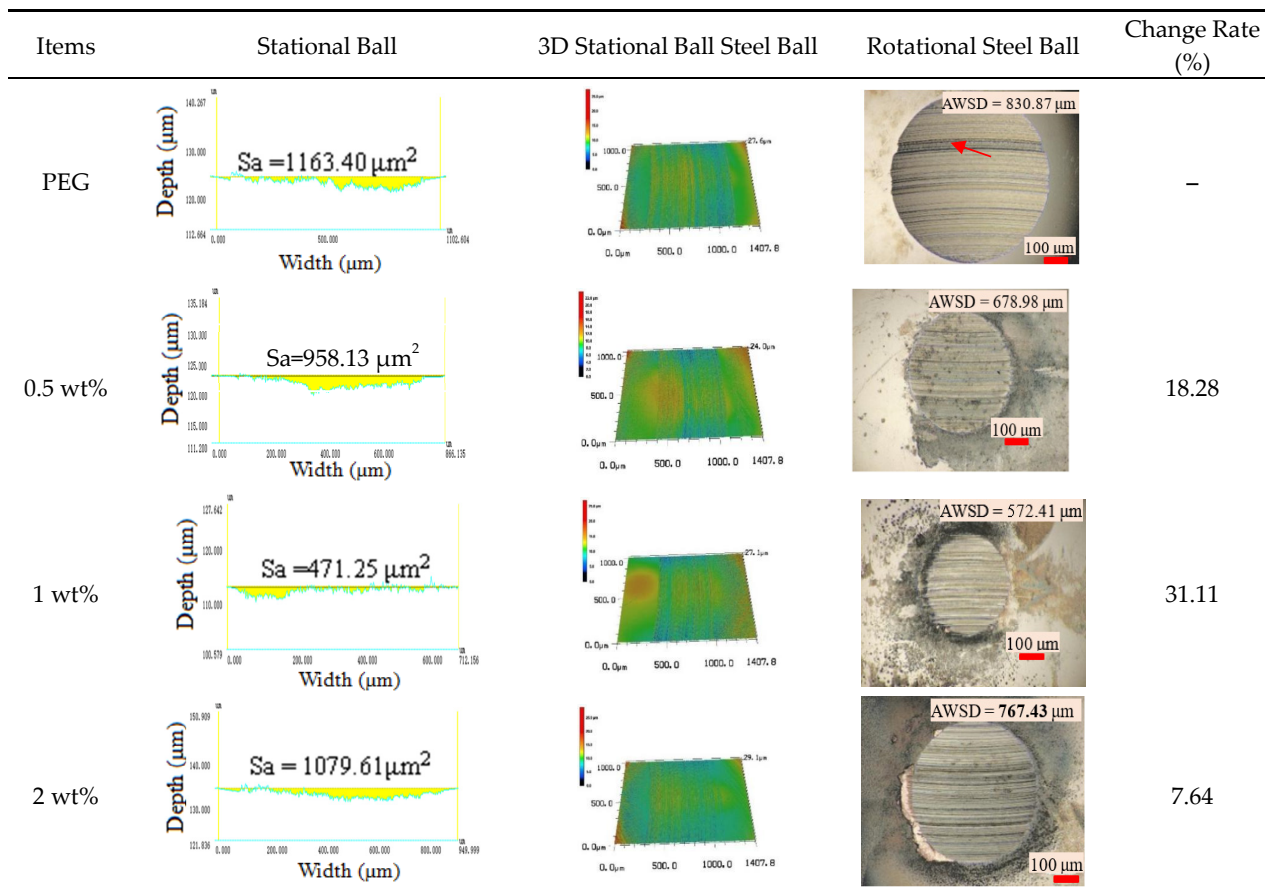
| Items | Stational Ball | 3D Stational Ball Steel Ball | Rotational Steel Ball | Change Rate (%) |
|---|---|---|---|---|
| PEG | Sa = 1163.40 µm² | | AWSD = 830.87 µm | – |
| 0.5 wt% | Sa = 958.13 µm² | | AWSD = 678.98 µm | 18.28 |
| 1 wt% | Sa = 471.25 µm² | | AWSD = 572.41 µm | 31.11 |
| 2 wt% | Sa = 1079.61 µm² | | AWSD = 767.43 µm | 7.64 |

**Figure 8.** Cross-sectional area, three-dimensional morphology, average wear scar diameter, and change rate of wear scar area lubricated by different oil samples at 100 °C.
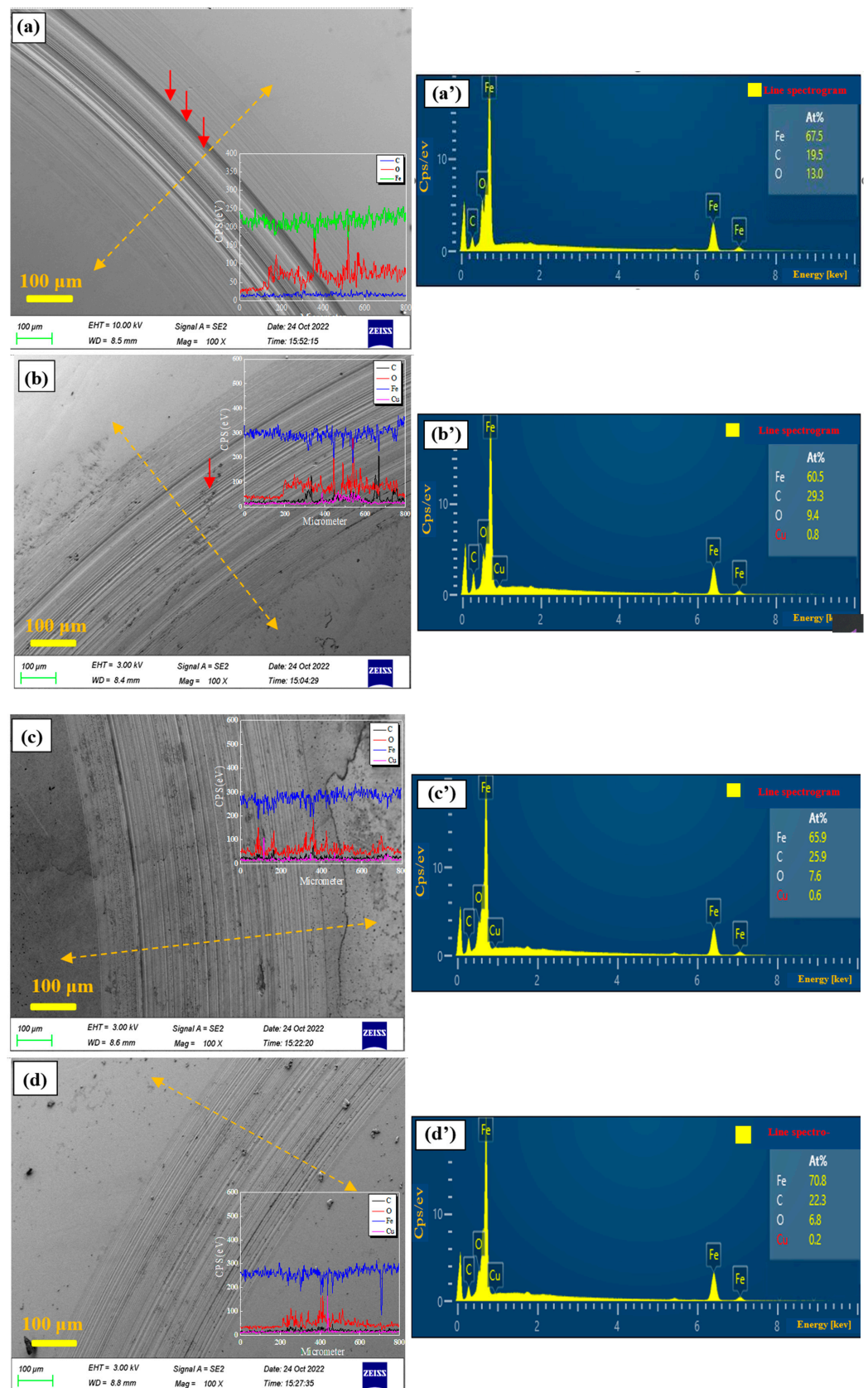
**Figure 9.** Surface wear scar morphology and energy spectrum analysis of steel ball lubricated by different content of copper-doped carbon, (**a**,**a'**) pure PEG, (**b**,**b'**) 0.5 wt% Cu-CQDs, (**c**,**c'**) 1.0 wt% Cu-CQDs, and (**d**,**d'**) 2.0 wt% Cu-CQDs.

*3.4. Analysis of Friction and Wear Mechanism*

Generally, the heat generated by friction will lead to the oxidation of lubricating oil, and the wear debris generated will also lead to further deterioration of the oil. PEG solution with different amounts of Cu-CQDs added was easy to oxidize under friction induction (Figure S3c), especially at high temperatures. The deterioration of oil products will reduce the anti-wear property of lubricating oil film. The mechanism of the lubricating performance of Cu-CQDs solution at high temperature was determined by heating the oil sample in an air blast drying oven at a certain temperature and time, and the influence of local high temperature generated at the steel ball interface during the friction process. A certain amount of Cu-CQDs solution was taken and heated to 100 °C from room temperature in an air blast drying oven. Cu-CQDs solution (2.0 wt%) was used to observe the colour change clearly. When the heating lasted for 30 min, the solution turned brick red, as shown in Figure S3b. When the solution was continuously heated or taken out of the oven for storage, the solution turned yellow again. This finding confirmed that the newly prepared 2.0 wt% Cu-CQDs produced cuprous ions when heated, but cuprous ions are not as stable as divalent copper ions in solution. The cuprous ion formed coordination compounds with water molecules in Cu-CQDs. The simulated experimental proves that the cuprous ion in solution will change into copper ion under high temperature and friction induce role.

According to the typical octahedral field and crystal field stabilization energy (CFSE) formed in the ligand field theory [35]. The energy reduction after Cu (II) coordination is relatively stable. However, the energy of Cu (I) is not stable, and the copper ion (Cu (II)) in the solution was more stable than that of copper ion (Cu (I)) [36]. When the solution was heated or taken out for standing, the unstable cuprous ion will self-disproportionate and transform into a more stable copper ion (Cu (II)). This conclusion can be used to explain the reason why the lubricity of PEG can be improved by the colour change of the oil sample during the friction process. After friction, black agglomerated CuO particles were found in the collected oil stain, indicating that the cuprous ions (Cu (I)) were oxidized to copper oxide (Cu (II)) at the interface of the friction pair during lubrication and participated in the formation of the boundary lubrication film. Figure 9 shows the EDS analysis in the wear scar area. The content of copper element increased significantly, confirming that copper oxides participated in the formation of boundary lubricating film.

The recognized lubrication mechanism of CQDs is the carbon film formed at the friction interface, and the C-σ bond passivation is related [37]. The SEM/EDS image in Figure 9 shows that the carbon content in the wear area after PEG lubrication containing Cu-CQDs (29.3 wt%) is significantly higher than that of pure PEG200 lubrication (19.5 wt%). This finding proves that Cu-CQDs additives can be rapidly deposited and embedded in the wear surface through physical absorption and electrostatic attraction [38]. With the increase in time, during the friction process, copper and trace cuprous oxide form copper derivatives on the surface of the friction pair. The continuous deposition of carbon at the interface forms a protective film (boundary friction film), thus reducing the direct contact between friction pairs and increasing the content of C and Cu. The composition of the boundary film can be illustrated by the valence states of each element in Figure 10. Figure 10a shows the general flow chart, indicating that Cu-CQDs induced by friction participate in the formation of the boundary film. Figure 10b shows the valence spectrum of carbon element (C1s) in the boundary film. The peak at 284.6 eV belongs to C-C or C-H in the film, and while the peak at 288 eV belongs to C-O. Figure 10c shows the chemical valence state of oxygen element (O1s) in the film. The peak at 529.4 eV belongs to iron oxide, while the peak at 532 eV belongs to ferric hydroxide [39]. Figure 10d shows the valence state of iron (Fe2p), confirming that iron oxides are Fe (706 eV), FeO, $Fe_2O_3$, and $Fe_3O_4$ (709–711 eV) [40,41]. Figure 10e shows the valence of copper (Cu LMM). The peak at 910 eV belongs to copper oxide, confirming that the friction induced copper-doped CQDs participate in the formation of boundary lubrication film, thus playing a good role in friction reduction and anti-wear. In addition, the low content of Cu-CQDs in PEG was dispersed uniformly which is easy to form the boundary lubrication film under friction process; however, the high content of

Cu-CQDs in PEG was easy to be agglomerated or wear debris resulted in abrasive wear. It could be proved by the aggregates in PEG after friction.
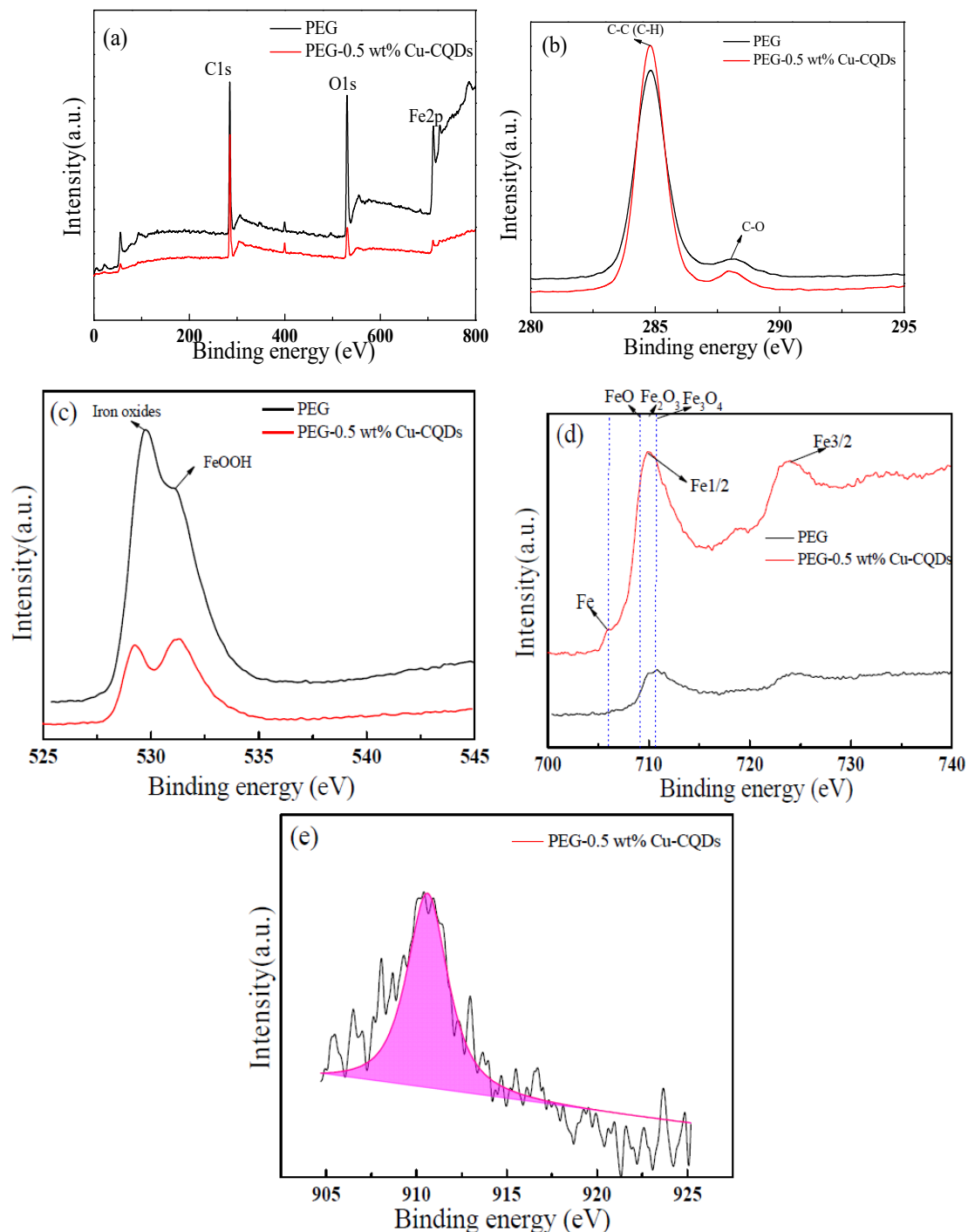


**Figure 10.** Valence analysis of different elements in the wear scar region of steel ball: (**a**) XPS total spectrum; (**b**) C1s; (**c**) O1s; (**d**) Fe$_{2p}$; and (**e**) Cu$_{2p}$.

## 4. Conclusions

High-performance lubricants for energy saving and reduced consumption were developed by preparing a novel copper-doped CQDs dispersion via hydrothermal synthesis. On the four-ball friction tester, the influence of copper-based CQD dispersion with different dosages on the lubrication performance of polyethylene glycol at different temperatures was investigated, and the following conclusions were obtained:

(1) The average particle size of the synthesized Cu-CQDs in the dispersion solution is about 8.33 nm, which shows good dispersion in PEG200.

(2) At the different test temperatures, the anti-wear and antifriction properties of PEG200 were significantly improved by adding 1.0 wt% Cu-CQDs dispersion.

(3) The friction and wear mechanism of Cu-CQDs dispersion can be attributed to the boundary lubrication film including the components of Cu-CQDs, thus reducing the friction and wear of the friction pair.

**Supplementary Materials:** The following supporting information can be downloaded at: https://www.mdpi.com/article/10.3390/lubricants11020086/s1, Figure S1: Fluorescence emission spectrum of Cu-CQDs; Figure S2: Infrared spectrogram analysis of CQDs and PEG (a) 1.0 wt%Cu-CQDs+PEG200; (b) pure Cu-CQDs; (c) PEG-200; Figure S3: (a) Agglomeration morphology of Cu-CQDs in PEG after friction; (b) Color of 2.0 wt% Cu-CQDs after passing through an air blast drying oven at 100 °C for 30 min; (c) Appearance color of oil stain at different temperatures of 2.0 wt% Cu-CQDs (1) 2.0 wt% Cu-CQDs, (2) 2.0 wt% Cu-CQDs at 25 °C, (3) 2.0 wt% Cu-CQDs at 75 °C, (4) 2.0 wt% Cu-CQDs at 100 °C.

**Author Contributions:** Methodology, S.L., K.H. and H.Z.; validation, S.L.; formal analysis, Y.C.; investigation, E.S.; data curation, X.Y. and J.W.; writing—original draft preparation, Y.X.; writing—review and editing, X.H.; supervision, E.H.; project administration, X.H. All authors have read and agreed to the published version of the manuscript.

**Data Availability Statement:** Not applicable.

**Conflicts of Interest:** The authors declare no conflict of interest.

# References

1. Xue, Q.; Liu, W.; Zhang, Z. Friction and wear properties of a surface-modified TiO$_2$ nanoparticle as an additive in liquid paraffin. *Wear* **1997**, *213*, 29–32. [CrossRef]

2. Wang, B.; Qiu, F.; Barber, G.C.; Zou, Q.; Wang, J.; Guo, S.; Yuan, Y.; Jiang, Q. Role of nano-sized materials as lubricant additives in friction and wear reduction: A review. *Wear* **2022**, *490*, 204206. [CrossRef]

3. Uflyand, I.E.; Zhinzhilo, V.A.; Burlakova, V.E. Metal-containing nanomaterials as lubricant additives: State-of-the-art and future development. *Friction* **2019**, *7*, 93–116. [CrossRef]

4. Han, K.; Zhang, Y.; Song, N. The Current Situation and Future Direction of Nanoparticles Lubricant Additives in China. *Lubricants* **2022**, *10*, 312. [CrossRef]

5. Zhang, Y. Energy efficiency techniques in machining process: A review. *Int. J. Adv. Manuf. Technol.* **2014**, *71*, 1123–1132.

6. He, Q.; Liu, H.; Ye, J. Tribological properties of nano copper as N32 lubricating oil additive. *Tribology* **2010**, *2*, 145–149. (In Chinese)

7. Qin, Y.; Wu, M.; Yang, Y.; Yang, Y.; Yang, G. Enhanced ability of halloysite nanotubes to form multilayer nanocrystalline tribofilms by thermal activation. *Tribol. Int.* **2022**, *174*, 107718. [CrossRef]

8. Jiang, H.; Hou, X.; Ma, Y.A.; Su, D.; Qian, Y.; Ahmed Ali, M.K.; Dearn, K.D. The tribological performance evaluation of steel-steel contact surface lubricated by polyalphaolefins containing surfactant-modified hybrid MoS$_2$/h-BN nano-additives. *Wear* **2022**, *504–505*, 204426. [CrossRef]

9. Lahouij, I.; Vacher, L.; Martin, J.; Dassenoy, F. IF-MoS$_2$ based lubricants: Influence of size, shape and crystal structure. *Wear* **2012**, *296*, 558–566. [CrossRef]

10. Li, B.; Xia, Y.; Wang, X. Friction and wear properties of nano Cu in polyethylene glycol solution. *Tribology* **2005**, *25*, 385–389. (In Chinese)

11. Zhu, S.; Song, Y.; Zhao, X. The photoluminescence mechanism in carbon dots (graphene quantum dots, carbon nanodots, and polymer dots): Current state and future perspective. *Nano Res.* **2015**, *8*, 355–381. [CrossRef]

12. Yang, Z.; Li, Z.; Xu, M.; Ma, Y.; Zhang, J.; Su, Y. Controllable synthesis of fluorescent carbon dots and their detection application as nanoprobes. *Nano-Micro Lett.* **2013**, *5*, 247–259. [CrossRef]

13. Kumar, V.B.; Sahu, A.K.; Rao, K.B.S. Development of Doped Carbon Quantum Dot-Based Nanomaterials for Lubricant Additive Applications. *Lubricants* **2022**, *10*, 144. [CrossRef]

14. Tang, W.; Zhang, Z.; Li, Y. Application of carbon spot in lubrication field: A review. *J. Mater. Sci.* **2021**, *56*, 12061–12092. [CrossRef]

15. Ma, W.; Gong, Z.; Gao, K. Superlubricity achieved by carbon quantum dots in ionic liquid. *Mater. Lett.* **2017**, *195*, 220–223. [CrossRef]

16. Shang, W.; Cai, T.; Zhang, Y.; Liu, D.; Sun, L.; Su, X.; Liu, S. Covalent grafting of chelated othoborate ionic liquid on carbon quantum dot towards high performance additives: Synthesis, characterization and tribological evaluation. *Tribol. Int.* **2018**, *121*, 302–309. [CrossRef]

17. Tang, J.; Chen, S.; Jia, Y.; Ma, Y.; Xie, H.; Quan, X.; Ding, Q. Carbon dots as an additive for improving performance in water-based lubricants for amorphous carbon (aC) coatings. *Carbon* **2020**, *156*, 272–281. [CrossRef]

18. Hu, Y.; Wang, Y.; Wang, C.; Ye, Y.; Zhao, H.; Li, J.; Xue, Q. One-pot pyrolysis preparation of carbon dots as eco-friendly nano-additives of water-based lubricants. *Carbon* **2019**, *152*, 511–520. [CrossRef]

19. He, J.; Sun, J.; Choi, J.; Wang, C.; Su, D. Synthesis of N-doped carbon quantum dots as lubricant additive to enhance the tribological behavior of MoS$_2$ nanofluid. *Friction* **2022**, *11*, 441–459. [CrossRef]

20. Ye, M.; Cai, T.; Zhao, L.; Liu, D. Covalently attached strategy to modulate surface of carbon quantum dots: Towards effectively multifunctional lubricant additives in polar and apolar base fluids. *Tribol. Int.* **2019**, *136*, 349–359. [CrossRef]

21. Tu, Z.; Hu, E.; Wang, B.; David, K.D.; Seeger, P.; Moneke, M.; Hu, X. Tribological behaviors of Ni-modified citric acid carbon quantum dot particles as a green additive in polyethylene glycol. *Friction* **2020**, *8*, 182–197. [CrossRef]

22. Huang, H.; Hu, H.; Qiao, S.; Bai, L.; Han, M.; Liu, Y.; Kang, Z. Carbon quantum dot/CuSx nanocomposites towards highly efficient lubrication and metal wear repair. *Nanoscale* **2015**, *7*, 11321–11327. [CrossRef] [PubMed]

23. Shang, W.; Cai, T.; Zhang, Y.; Liu, D.; Liu, S. One pot pyrolysis synthesis of carbon quantum dots and graphene oxide nanomaterials: All carbon hybrids as eco-environmental lubricants for low friction and remarkable wear-resistance. *Tribol. Int.* **2018**, *118*, 373–380. [CrossRef]

24. Wang, F.; Shang, L.; Zhang, G.; Wang, Z. Polyethylene glycol derived carbon quantum dots nanofluids: An excellent lubricant for diamond-like carbon film/bearing steel contact. *Friction* **2022**, *10*, 1393–1404. [CrossRef]

25. De, B.; Karak, N. A green and facile approach for the synthesis of water soluble fluorescent carbon dots from banana juice. *RSC Adv.* **2013**, *3*, 8286–8290. [CrossRef]

26. Gao, S.; Chen, Y.; Fan, H.; Wei, X.; Hu, C.; Wang, L.; Qu, L. A green one-arrow-two-hawks strategy for nitrogen-doped carbon dots as fluorescent ink and oxygen reduction electrocatalysts. *J. Mater. Chem. A* **2014**, *2*, 6320–6325. [CrossRef]

27. Hu, E.; Hu, K.; Dearn, K.D.; Hu, X.; Xu, Y.; Yu, D.; Tang, Y. Tribological performance of rice husk ceramic particles as a solid additive in liquid paraffin. *Tribol. Int.* **2016**, *103*, 139–148. [CrossRef]

28. Cai, J.; Dai, L. Study on the method for measuring the friction coefficient of lubricating oil (four ball method). *Lubr. Oil* **2001**, *16*, 5. (In Chinese)

29. Odi-Owei, S.; Roylance, B.J.; Xie, L. An experimental study of initial scuffing and recovery in sliding wear using a four-ball machine. *Wear* **1987**, *117*, 267–287. [CrossRef]

30. Ke, L.; Wang, Y. Two-dimensional sliding frictional contact of functionally graded materials. *Eur. J. Mech.-A Solids* **2007**, *26*, 171–188. [CrossRef]

31. Davey, W.; Edwards, E.D. The extreme-pressure lubricating properties of some sulphides and disulphides, in mineral oil, as assessed by the Four-Ball Machine. *Wear* **1958**, *1*, 291–304. [CrossRef]

32. Sarno, M.; Mustafa, W.A.A.; Senatore, A.; Scarpa, D. One-step "green" synthesis of dispersable carbon quantum dots/poly (methyl methacrylate) nanocomposites for tribological applications. *Tribol. Int.* **2020**, *148*, 106311. [CrossRef]

33. Wen, S.; Huang, P. *Principles of Tribology*; Tsinghua University Press: Beijing, China, 2002.

34. Sato, H.; Tokuoka, N.; Yamamoto, H.; Sasaki, M. Study on Wear Mechanism by Soot Contaminated in Engine Oil (First report: Relation between Characteristics of Used Oil and Wear). *SAE Tech. Pap.* **1999**, *1*, 3573.

35. Wang, J.; Cui, J.; Wang, X.; Qin, X. *Inorganic Chemistry*, 5th ed.; Higher Education Press: Beijing, China, 2018. (In Chinese)

36. Xia, J.; Tang, D. Preparation, characterization and catalytic performance of copper ion intercalated graphite oxide composites. *New Chem. Mater.* **2011**, *39* (Suppl. S1), 85–89. (In Chinese)

37. Mou, Z.; Wang, B.; Lu, H.; Quan, H.; Huang, Z. Branched polyelectrolyte grafted carbon dots as the high-performance friction-reducing and antiwear additives of polyethylene glycol. *Carbon* **2019**, *149*, 594–603. [CrossRef]

38. Wang, J.; Li, X.; Deng, Y.; Chen, S.; Liang, W.; Zhang, L.; Wan, Y. Carbon quantum dots doped with silver as lubricating oil additive for enhancing tribological performance at various temperatures. *Appl. Surf. Sci.* **2022**, *599*, 154029. [CrossRef]

39. Chen, Y.; Hu, E.; Zhong, H.; Wang, J.; Subedi, A.; Hu, K.; Hu, X. Characterization and tribological performances of graphene and fluorinated graphene particles in PAO. *Nanomaterials* **2021**, *11*, 2126. [CrossRef] [PubMed]

40. Hu, E.; Dearn, K.; Yang, B.; Song, R.; Xu, Y.; Hu, X. Tribofilm formation and characterization of lubricating oils with biofuel soot and inorganic fluorides. *Tribol. Int.* **2017**, *107*, 163–172. [CrossRef]

41. Hu, E.; Hu, K.; Xu, Y.; Hu, X.; Chen, D.; Cheng, Z.; Wu, D. Study on the mechanism of friction induced changes in the composition and structure of soot particles from biofuels. *Tribology* **2016**, *36*, 185–193. (In Chinese)